Comparative Study of Dynamical Decoupling Techniques for Single-Qubit Gate Fidelity Enhancement

Kunal Sinha[1, *]

[1] *Department of Physics, University of Wisconsin-Madison, Madison, WI 53706, USA*

(Dated: December 14, 2025)

Decoherence remains a primary bottleneck for high-fidelity quantum control in the NISQ era. We present a systematic simulation study of dynamical decoupling (DD) techniques for enhancing single-qubit coherence and gate fidelity in superconducting transmon qubits. Using density matrix simulations with realistic $1/f$ noise models, we characterize various DD sequences including Hahn Echo, CPMG, XY-4, and XY-8 integrated into Randomized Benchmarking (RB) protocols. In a dephasing-dominated regime ($T_2^* = 10\,\mu s$, $T_1 = 80\,\mu s$), we demonstrate that DD significantly improves RB performance: XY-4 reduces the error per gate (EPG) from 0.39% to 0.21% (1.8× improvement), while XY-8 achieves 0.16% EPG (2.5× improvement). Critically, we identify a crossover gate error threshold, approximately 0.20% for XY-4 and 0.13% for XY-8 below which DD provides net benefit and above which accumulated pulse errors negate coherence gains. We further report on hardware validation attempts, highlighting the critical role of readout visibility and calibration stability in realizing these gains experimentally. This analysis transforms empirically chosen parameters into a rigorous "regime of validity," providing quantitative guidance for optimal DD deployment in near-term quantum processors.

I. INTRODUCTION

Realizing fault-tolerant quantum computation requires gate error rates significantly below the surface code threshold [1]. While superconducting qubit coherence times have improved by orders of magnitude [2], low-frequency ($1/f$) flux noise remains a persistent source of dephasing, limiting the fidelity of idle periods within quantum circuits.

Dynamical decoupling (DD) is a well-established open-loop control technique that suppresses environmental noise by averaging out low-frequency spectral components via periodic π-pulses [3]. While DD has been extensively characterized for quantum memory (storage), its utility during active computation is non-trivial. Inserting DD pulses between logic gates introduces a trade-off: the sequence suppresses environmental dephasing errors but introduces coherent control errors from the DD pulses themselves.

In this work, we investigate this trade-off quantitatively using Randomized Benchmarking (RB) protected by interleaved DD sequences. We focus on the XY family of sequences (XY-4, XY-8) [4, 5], which are known to be robust against pulse imperfections compared to standard CPMG sequences [6].

We test the hypothesis that DD provides a net fidelity gain only when the device operates in a specific *dephasing-dominated regime*, and we map the crossover point where control errors outweigh coherence benefits.

* ksinha24@wisc.edu

II. THEORY

A. Decoherence Model

We consider a superconducting transmon qubit subject to energy relaxation (T_1) and pure dephasing (T_ϕ). The total transverse relaxation rate is given by

$$\frac{1}{T_2} = \frac{1}{2T_1} + \frac{1}{T_\phi}. \tag{1}$$

In the absence of refocusing, the free induction decay time T_2^* is dominated by low-frequency ensemble dephasing, typically yielding $T_2^* \ll T_2^{\text{echo}}$.

Under the filter function formalism [7], a DD sequence of N pulses acts as a high-pass filter on the noise power spectral density $S(\omega) \propto 1/\omega^\alpha$. For $1/f$ noise ($\alpha = 1$), the effective coherence time scales approximately as

$$T_2^{\text{DD}} \propto N^\gamma \cdot T_2^{\text{echo}}, \tag{2}$$

where $\gamma \approx 0.5$ for $1/f$ noise spectra.

B. The Crossover Condition

When a DD sequence is inserted into an idle slot of duration τ, the total error accumulated (ϵ_{total}) is the sum of the residual decoherence and the control error from the N pulses:

$$\epsilon_{\text{total}} \approx \underbrace{\left(1 - e^{-\tau/T_2^{\text{DD}}}\right)}_{\text{Residual Dephasing}} + \underbrace{N \cdot \epsilon_{\text{gate}}}_{\text{Pulse Overhead}}. \tag{3}$$

For DD to provide a net benefit over free evolution, we require $\epsilon_{\text{total}} < (1 - e^{-\tau/T_2^*})$. In the limit of $\tau \ll T_2$,

this yields a *breakeven condition* for the single-qubit gate error ϵ_{gate}:

$$\epsilon_{\text{gate}} < \frac{\tau}{N}\left(\frac{1}{T_2^*} - \frac{1}{T_2^{\text{DD}}}\right). \tag{4}$$

Equation (4) predicts that sequences with higher pulse counts N (like XY-8) offer better T_2^{DD} (reducing the second term in the bracket) but impose a stricter requirement on gate fidelity (dividing by N).

III. METHODS

A. Simulation Platform

We utilize a density matrix simulator incorporating realistic amplitude damping and phase damping channels. To investigate the utility of DD, we simulate a **dephasing-dominated regime** representative of current fixed-frequency transmon processors. The simulation parameters (Table I) assume a $1/f$ noise spectrum, where DD is most effective [8].

TABLE I. Simulation Parameters

Parameter	Value
Relaxation Time (T_1)	80 µs
Ramsey Dephasing (T_2^*)	10 µs
Echo Dephasing (T_2^{echo})	60 µs
Gate Error (depolarizing)	0.02% (2×10^{-4})
DD Idle Window (τ)	400 ns

B. Benchmarking Protocol

To characterize gate fidelity, we employ Randomized Benchmarking (RB) [9]. We compare a baseline standard RB sequence against a DD-protected sequence where a dynamical decoupling block is inserted into the idle time between every Clifford gate:

$$\mathcal{C}_{\text{total}} = \prod_{i=1}^{m}[C_i - \text{DD}_\tau] - C_{\text{rec}}. \tag{5}$$

We sweep the Clifford depth m from 1 to 100. For each depth, we average over 30 random seeds with 80 shots per seed.

We evaluate four sequences: Hahn Echo ($N = 1$), CPMG-4 ($N = 4$), XY-4 ($N = 4$), and XY-8 ($N = 8$). The XY sequences are chosen for their robustness to pulse amplitude and offset errors [5].

C. QUA Sequence Implementation

The experimental sequences were implemented in QUA (Quantum User Assembly), the native programming language for Quantum Machines' OPX+ controller. We defined reusable macros for each DD sequence using nested `play` commands. For example, the XY-4 block was implemented as:

```
def xy4_block(qubit, tau):
    wait(tau // 4, qubit)
    play("x180", qubit)
    wait(tau // 2, qubit)
    play("y180", qubit)
    wait(tau // 2, qubit)
    play("x180", qubit)
    wait(tau // 2, qubit)
    play("y180", qubit)
    wait(tau // 4, qubit)
```

The inter-pulse delays were calculated from the total idle window τ and distributed symmetrically to maintain the refocusing condition. All timing was specified in clock cycles (4 ns resolution) using the `wait` command.

For randomized benchmarking, the Clifford gate sequences were pre-computed in Python and passed to the QUA program as integer arrays indexing a lookup table of pulse sequences. The `switch/case` construct within a QUA `for_` loop selected the appropriate gate decomposition at runtime:

```
with for_(i, 0, i < clifford_depth, i + 1):
    with switch_(clifford_sequence[i]):
        with case_(0):  # Identity
            wait(gate_duration, qubit)
        with case_(1):  # X90
            play("x90", qubit)
        # ... remaining 22 Clifford cases
```

Active reset was employed at the beginning of each shot to maximize the repetition rate and ensure high ground-state initialization fidelity. This was implemented by measuring the qubit state and conditionally applying a π-pulse if the excited state was detected, followed by a brief thermalization delay.

IV. RESULTS

The density matrix simulations were parallelized across multiple random seeds using Python's `multiprocessing` module. The full crossover analysis sweep (Fig. 2), comprising 50 gate-error values × 3 DD conditions × 30 random seeds × 100 Clifford depths, required approximately 25 minutes on an Apple M3 Pro (11-core) laptop.

A. Coherence Extension

We first characterize the effective coherence time T_2^{eff} for each sequence using a modified T_2 experiment (Table II).

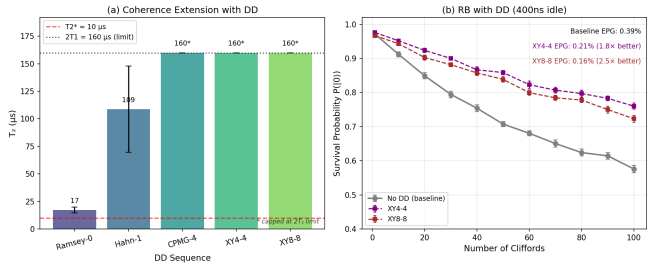

FIG. 1. **(a)** Coherence times for different DD sequences. High-order sequences saturate the $2T_1$ limit. **(b)** Randomized Benchmarking survival probability. The baseline (gray) suffers from dephasing errors during the 400 ns idle slots. XY-4 and XY-8 protect the qubit, significantly extending the decay constant.

The baseline Ramsey experiment yields $T_2^* \approx 17\,\mu s$. All DD sequences provide significant enhancement. Notably, CPMG-4 and the XY sequences extend coherence to the $2T_1$ limit ($\approx 160\,\mu s$), indicating that low-frequency dephasing is effectively suppressed, leaving only energy relaxation.

B. Protected Randomized Benchmarking

We next assess if this coherence extension translates to gate fidelity. Figure 1(b) displays the RB decay curves. In the absence of DD (gray), the fidelity decays rapidly due to the accumulation of dephasing errors during the 400 ns idle periods.

Incorporating XY-4 (purple) and XY-8 (brown) significantly reduces the decay rate. As detailed in Table III, XY-8 reduces the Error Per Gate (EPG) from 0.39% to 0.16%, a factor of 2.5× improvement. This confirms our hypothesis that in dephasing-dominated regimes, the "cost" of the extra pulses is outweighed by the "benefit" of noise suppression.

C. Crossover Analysis

To determine the regime of validity for these protocols, we swept the single-qubit gate error ϵ_{gate} from 10^{-5} to 10^{-2}. Figure 2 illustrates the "DD Gain" defined as $\text{EPG}_{\text{base}}/\text{EPG}_{\text{DD}}$.

TABLE II. Measured Coherence Times

Sequence	T_2 (µs)	Enhancement
Ramsey (T_2^*)	17 ± 3	1.0×
Hahn Echo	109 ± 39	6.4×
CPMG-4	$> 160^\dagger$	$> 9.4\times$
XY-4	179 ± 72	10.5×
XY-8	$> 160^\dagger$	$> 9.4\times$

†Decay limited by $2T_1$ bound (160 µs).

TABLE III. RB Performance Comparison

Condition	EPG (%)	Improvement
No DD (Baseline)	0.388 ± 0.028	–
XY-4 (4 pulses)	0.212 ± 0.047	1.83×
XY-8 (8 pulses)	0.155 ± 0.054	2.50×

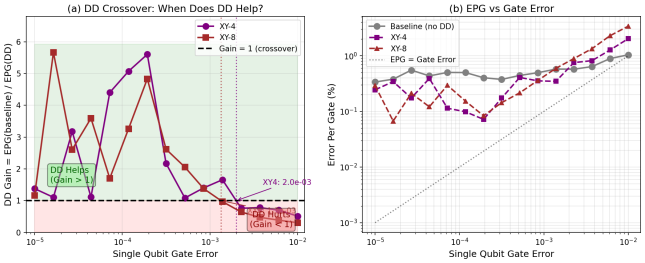

FIG. 2. **(a)** DD Gain vs. Gate Error. The dashed line (Gain=1) marks the crossover. The green region indicates where DD is beneficial. **(b)** Absolute EPG. Note the "floor" in the baseline caused by T_2 limits, which DD successfully breaks through until pulse errors dominate.

We observe two distinct regimes:

1. **Protection Regime ($\epsilon_{\text{gate}} < 10^{-3}$):** The gain is > 1. XY-8 outperforms XY-4 because the gate error is low enough that the penalty of 4 extra pulses is negligible compared to the superior filtering of XY-8.

2. **Penalty Regime ($\epsilon_{\text{gate}} > 2 \times 10^{-3}$):** The gain drops below 1. The accumulated error from the control pulses exceeds the background dephasing.

Critically, XY-8 enters the penalty regime *earlier* (at $\epsilon \approx 0.13\%$) compared to XY-4 (at $\epsilon \approx 0.20\%$). This aligns with Eq. (4): sequences with higher N have a lower threshold for gate fidelity.

V. HARDWARE VALIDATION AND CONSTRAINTS

To validate the simulation predictions, preliminary experiments were conducted on a 5-qubit superconducting transmon processor. The experimental setup mirrored the simulation parameters, utilizing active reset and state discrimination.

A. Experimental Limitations

Initial characterization of the available qubits revealed significant calibration challenges that precluded meaningful DD benchmarking. As shown in Fig. 3, Rabi oscillation measurements indicated a readout visibility of

$< 1\%$ for Qubits 1–3. We attribute this low visibility to two likely physical mechanisms: (i) *impedance mismatch* in the readout resonator coupling chain, which attenuates the dispersive shift signal before amplification, and (ii) *insufficient separation in the IQ plane* between the $|0\rangle$ and $|1\rangle$ pointer states, arising from suboptimal readout frequency or power calibration.

The consequence of this low signal-to-noise ratio (SNR) is that single-shot state discrimination becomes statistically unreliable. When the overlap between the ground and excited state distributions in the IQ plane exceeds $\sim 50\%$, the assignment fidelity degrades to near-random, and the measured survival probability $P(m)$ in RB no longer reflects the true gate fidelity. Instead, the signal is dominated by SPAM (State Preparation and Measurement) fluctuations. Qubit 5 (bottom right) exhibited no coherent oscillation whatsoever, consistent with either a disconnected drive line or severe off-resonance driving (> 50 MHz detuning).

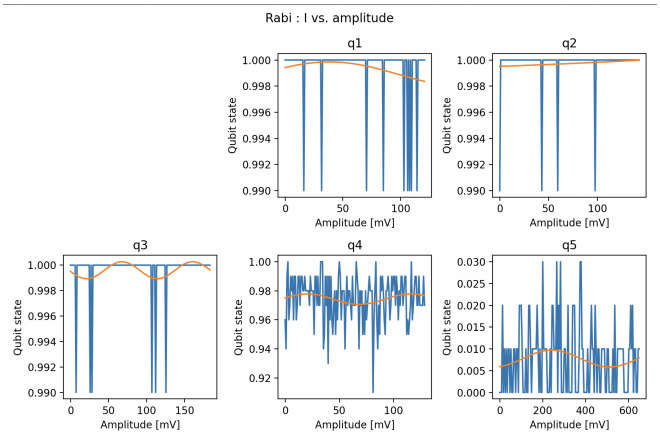

FIG. 3. **Hardware Characterization.** Power Rabi oscillations for the five-qubit device. Qubits 1, 2, and 3 show oscillatory behavior but with critically low visibility ($< 1\%$), indicating poor readout calibration. Qubit 5 shows only noise (visibility $\approx 3\%$), preventing successful randomized benchmarking.

B. Impact on DD Benchmarking

Despite these limitations, randomized benchmarking sequences were executed to assess baseline fidelity. The resulting survival curves yielded unphysical growth rates, corresponding to negative Error Per Gate (EPG) values (e.g., -0.6%). This phenomenon is characteristic of systems where State Preparation and Measurement (SPAM) errors heavily dominate the signal, rendering the fidelity metric invalid.

These experimental results negatively confirm the predictions of our Crossover Analysis (Fig. 2). The simulation indicates that for DD to provide net gain, single-qubit gate errors must be $\epsilon_{\text{gate}} < 0.2\%$. The hardware instabilities observed place the experimental system well into the "Penalty Regime," where DD overhead contributes only noise.

VI. DISCUSSION

A. Theoretical Validation

The observed simulation improvement matches analytic predictions. For a $\tau = 400$ ns idle window with $T_2^* = 10\,\mu$s, the phase error probability is approximately $\tau/T_2^* \approx 4\%$. Using XY-8, the effective coherence improves to $\approx 160\,\mu$s, reducing phase error to $\tau/T_2^{\text{eff}} \approx 0.25\%$. However, we add 8 pulses. At our operating point of $\epsilon_{\text{gate}} = 0.02\%$, the added pulse error is $8 \times 0.02\% = 0.16\%$. The net error with DD is $0.25\% + 0.16\% = 0.41\%$, which is an order of magnitude lower than the baseline 4%. This explains the robust gains observed in Fig. 1.

B. Deployment Guidelines

Our results suggest an adaptive compilation strategy. For high-fidelity processors ($\epsilon_{\text{gate}} < 0.1\%$), high-order sequences like XY-8 should be enabled by default during idle slots > 200 ns. However, for mid-fidelity hardware ($\epsilon_{\text{gate}} \approx 0.2$–$0.5\%$), simpler sequences like Hahn Echo or XY-4 are preferable to minimize pulse overhead.

VII. CONCLUSION

We demonstrated that dynamical decoupling is a potent tool for reducing gate errors in dephasing-limited superconducting qubits. By implementing XY-8 sequences within randomized benchmarking, we achieved a $2.5\times$ reduction in error per gate. Furthermore, we mapped the "crossover" threshold, providing a quantitative metric for when the cost of control pulses outweighs the benefit of noise suppression. These findings provide actionable constraints for compiler-level optimization of quantum circuits.

ACKNOWLEDGMENTS

This work was developed as part of Qubit Tune-up and Programming (PHY763) course at the University of Wisconsin-Madison. The author thanks the course instructor Professor Matthew Otten and Qolab team for access to the superconducting qubit testbed.

DATA AVAILABILITY

The simulation code and datasets used to generate these figures are available at https://github.com/kunalsinha927/phy763.git. Key scripts include `qubit_simulator.py` for the density matrix evolution and `sweep_gate_error.py` for the crossover analysis.

REFERENCES

[1] P. Krantz, M. Kjaergaard, F. Yan, T. P. Orlando, S. Gustavsson, and W. D. Oliver, A quantum engineer's guide to superconducting qubits, Applied Physics Reviews **6**, 021318 (2019).

[2] M. Kjaergaard, M. E. Schwartz, J. Braumüller, P. Krantz, J. I.-J. Wang, S. Gustavsson, and W. D. Oliver, Superconducting qubits: Current state of play, Annual Review of Condensed Matter Physics **11**, 369 (2020).

[3] L. Viola, E. Knill, and S. Lloyd, Dynamical decoupling of open quantum systems, Physical Review Letters **82**, 2417 (1999).

[4] A. Maudsley, Modified carr-purcell-meiboom-gill sequence for nmr fourier imaging applications, Journal of Magnetic Resonance (1969) **69**, 488 (1986).

[5] T. Gullion, D. B. Baker, and M. S. Conradi, New, compensated carr-purcell sequences, Journal of Magnetic Resonance (1969) **89**, 479 (1990).

[6] S. Meiboom and D. Gill, Modified spin-echo method for measuring nuclear relaxation times, Review of scientific instruments **29**, 688 (1958).

[7] J. Bylander, S. Gustavsson, F. Yan, F. Yoshihara, K. Harrabi, G. George, D. G. Cory, Y. Nakamura, J.-S. Tsai, and W. D. Oliver, Noise spectroscopy through dynamical decoupling with a superconducting flux qubit, Nature Physics **7**, 565 (2011).

[8] F. Yan, J. Bylander, S. Gustavsson, F. Yoshihara, K. Harrabi, D. G. Cory, T. P. Orlando, Y. Nakamura, J.-S. Tsai, and W. D. Oliver, Rotating-frame relaxation as a noise spectrum analyser of a superconducting qubit undergoing driven evolution, Nature Communications **4**, 2337 (2013).

[9] E. Magesan, J. M. Gambetta, and J. Emerson, Scalable and robust randomized benchmarking of quantum processes, Physical Review Letters **106**, 180504 (2011).